ULTRASONIC DETECTION OF PLASTIC YIELDING IN STEEL SPECIMENS

Z. Radakovic and K. Willam
CEAE Department
University of Colorado at Boulder
Boulder, CO 80309-0428

L. J. Bond
Center for Acoustics, Mechanics and Materials
University of Colorado at Boulder
Boulder, CO 80309-0427

INTRODUCTION

In the case of localization the loss of ellipticity is synonymous with the formation of weak discontinuities, or jumps of the velocity gradients (strain rates). The singularity in the localization tensor indicates discontinuous bifurcation when jump conditions in static problems are examined. By analogy, the singularity in the acoustic tensor indicates loss of hyperbolicity, which is synonymous with zero wave propagation velocities in dynamic problems.

It is this analogy between the localization tensor and the acoustic tensor which led us to examine zero wave propagation properties for characterizing localized failure processes. Ultrasonic measurements of signal arrival times and amplitudes were performed on flat steel specimens, loaded in direct tension into the plastic yield regime. The objective was the characterization of discontinuous failure modes using ultrasonic wave measurements.

In this paper preliminary results from the longitudinal, shear, and Rayleigh wave experiments are presented.

ANALOGY BETWEEN LOCALIZATION AND ACOUSTIC ANALYSIS

In the following we review the background material of elastic and elasto-plastic analysis and its implications with regard to wave propagation.

Linear Elasticity

The general format of the localization/acoustic tensor in index notation is:

$$Q_{jl} = N_i E_{ijkl} N_k \ , \tag{1}$$

where E_{ijkl} denotes the elasticity tensor, and where the vector N_j, with $j = 1, 2, 3$, defines the normal of the discontinuity surface associated with plane acceleration waves. In the case of isotropic linear elastic solids, the expression in Eq. 1 reduces to the simplified form $Q_{jl} = (\lambda + \mu) N_i N_k + \mu \delta_{ik}$ which expands into:

$$\left[Q_{jl} \left\{ \begin{array}{c} N_1 \\ N_2 \\ N_3 \end{array} \right\} \right] = \left[\begin{array}{ccc} (\lambda+\mu)N_1^2 + \mu & (\lambda+\mu)N_1N_2 & (\lambda+\mu)N_1N_3 \\ (\lambda+\mu)N_1N_2 & (\lambda+\mu)N_2^2 + \mu & (\lambda+\mu)N_2N_3 \\ (\lambda+\mu)N_1N_3 & (\lambda+\mu)N_2N_3 & (\lambda+\mu)N_3^2 + \mu \end{array} \right] . \tag{2}$$

In this expression λ and μ denote the Lamé's parameters, N_1, N_2, N_3 the components of the propagation direction, and δ the Kronecker delta.

Review of Progress in Quantitative Nondestructive Evaluation, Vol. 14
Edited by D.O. Thompson and D.E. Chimenti, Plenum Press, New York, 1995

With isotropy, the eigenvalues of the linear elastic acoustic tensor are the same for any propagation direction:

$$\lambda(Q_{jl})=[\ \mu,\quad \mu,\quad \lambda+2\mu\ ]\ .$$

The elastic wave speeds are normally classified into transverse, quasi-transverse and quasi-longitudinal velocities, where

$$c_t=\sqrt{\frac{\mu}{\rho}}\ ,\qquad c_{qt}=\sqrt{\frac{\mu}{\rho}}\ ,\qquad c_{ql}=\sqrt{\frac{(\lambda+2\mu)}{\rho}}\ . \tag{3}$$

The corresponding eigenvectors define the polarization of the particle motion by the vector M_j, with $j=1,2,3$.

$$[M_j]^t=[N_2,-N_1,0],\quad [M_j]^{qt}=[0,N_3,-N_2],\quad [M_j]^{ql}=[N_1,N_2,N_3]\ . \tag{4}$$

The terminology quasi-longitudinal and quasi-transverse indicates that in anisotropic media the distinction between pure longitudinal and transverse waves does no longer exist.

Elasto-plasticity

The tangential material operator of non-associated elasto-plasticity written in index notation is:

$$E^{ep}_{ijkl}=E_{ijkl}-\frac{E_{ijst}m_{st}n_{pq}E_{pqkl}}{h+n_{pq}E_{pqrs}m_{rs}}\ , \tag{5}$$

where $n_{ij}=\frac{\partial F}{\partial\sigma_{ij}}$ denotes the gradient of the yield function $F(\sigma_{ij},q_i)=0$, and $m_{ij}=\frac{\partial Q}{\partial\sigma_{ij}}$ the gradient of the plastic potential $Q=Q(\sigma_{ij})$. In our notation $h=h(q_i)$ denotes the hardening/softening modulus which is positive for hardening, zero for elastic-perfectly plastic behavior and negative for softening.

Localization Analysis for Elastic Perfectly Plastic Solids

The onset of spatial discontinuities may be detected either through the kinematic argument of jump conditions, or the dynamic argument of stationary waves. In the first approach, the formation of a weak discontinuity in the velocity gradient is expressed in terms of a singularity of the localization tensor. The balance of linear momentum together with Maxwell's compatibility condition across discontinuity surfaces leads to the eigenproblem,

$$\dot{t}^+_j-\dot{t}^-_j=\dot{\gamma}\ Q_{jl}{}^{ep}\ M_l=0\ ,\quad \textit{where}\quad Q^{ep}_{jl}=\ N_iE^{ep}_{ijkl}\ N_k\ . \tag{6}$$

In this expression $\dot{t}^+_j,\dot{t}^-_j$ denote the rates of surface tractions on the positive and negative face respectively, $\dot{\gamma}$ the undefined amplitude of the jump, and M_l the direction of polarization.

In the second approach the concept of wave propagation views the formation of a spatial discontinuity as a stationary wave front condition when the phase velocity diminishes to zero. In other terms, when the propagation velocity of the discontinuous acceleration field vanishes for a certain polarization direction, then the zero wave propagation criterion reduces to

$$Q^{ep}_{jl}M_l=\rho c^2M_j\quad\text{with}\quad \rho c^2_{crit}\to 0\ . \tag{7}$$

This states that the quadratic form $M_j\ Q^{ep}_{jl}\ M_l$ must vanish for the case of a standing wave. For an elastic plastic Huber-Mises solid an analytic expression for the three wave velocities was developed in [5] for plastic yielding in uniaxial tension:

$$\frac{\rho c^2_t}{\mu}=1\ . \tag{8}$$

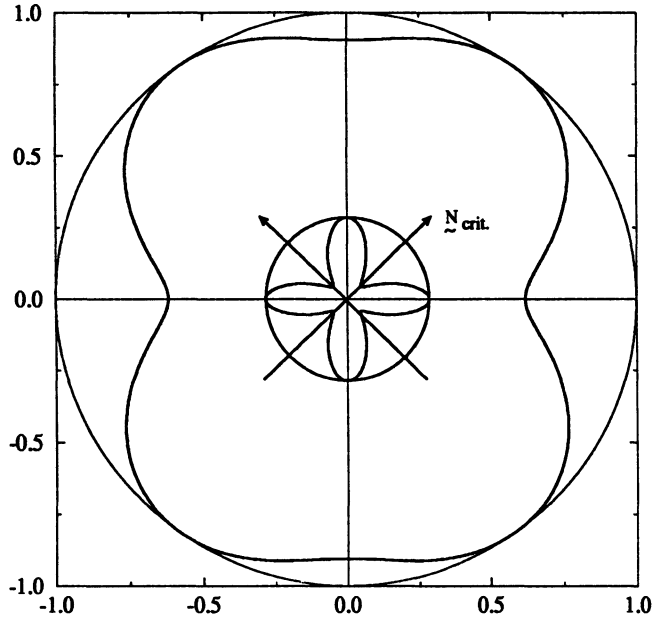

Figure 1: Polar plot of wave velocities in an elastic perfectly plastic Huber-Mises solid which is subjected to uniaxial tension, with Poisson's ratio = 0.3 normalized in the form $(\frac{c_{ql(t)}}{c_{ql}^{el}})^2$.

$$\left\{ \begin{array}{c} \frac{\rho c_{ql}^2}{\mu} \\ \frac{\rho c_{qt}^2}{\mu} \end{array} \right\} = \frac{1}{2} \left\{ \frac{3-4\nu}{1-2\nu} - \frac{3N_1^2+1}{3+(h/\mu)} \pm \sqrt{\left(\frac{1}{1-2\nu} + \frac{3N_1^2+1}{3+(h/\mu)} \right)^2 - \frac{4(3N_1^2-1)^2}{(3+(h/\mu))(1-2\nu)}} \right\}. \tag{9}$$

The three-dimensional analysis shows that transverse wave speed is not affected by the plastic flow, while the other two wave speeds show strong dependence on the plastic modulus h, the elastic shear modulus μ and Poisson's ratio ν, as well as on the direction of wave propagation N_1, N_2. The effect of plastic flow on velocity is illustrated best in the form of polar plots shown in Fig. 1 which depict the variation of the quasi-longitudinal and quasi-transverse wave speeds for $h = 0$. These polar diagrams are related to the slowness surfaces in ultrasonics [2] which plot the reciprocal values of phase velocities as a function of the propagation direction. The form of the polar plots depends strongly on the yield condition in the underlying plasticity model [7]. In fact, the initial intent in this study was to characterize the plastic yield condition using ultrasonic measurements of the polar phase velocities along different directions. The polar plots shown in Fig. 1 depict the two wave speeds which are normalized with regard to the longitudinal wave velocity of isotropic elasticity. The plots illustrate that plastic yielding in direct tension is responsible for stress induced anisotropy. For the 3-dim. case the shear wave velocity does not diminish to zero for perfectly plastic behavior, opposite to the case of plane stress where $\rho c_{qt}^2 = 0$ for $h = 0$ at the critical angle $\alpha = 35.26^o$. In 3-dim. analysis a strain softening modulus of $h = -E/12$ would be required to reduce the quasi-transverse wave speed to zero in the critical propagation direction where $N_1/N_2 = 0.74/0.67$ ($\alpha = 41.2^o$ for $\nu = 0.3$).

ULTRASONIC EXPERIMENTS

The ultrasonic experiments were performed on mild steel specimens which were loaded in direct tension into the plastic yield regime and then to ductile fracture.

Test Specimens and Instrumentation

Uniaxial tension experiments were performed on two types of prismatic specimens in the form of thick and thin flat bars. The thick specimens were 5.08 *cm* wide, 1.91 *cm* thick and 40.64 *cm* long. The thin specimens were 3.50 *cm* wide, 0.47 *cm* thick and 43.18 *cm* long. The shape of the specimen is shown schematically in Fig. 2. Quasi-longitudinal and quasi-transverse shear wave velocities were measured on the thick specimens, while Rayleigh wave experiments were performed on both types of specimens. The compression wave velocities were measured using 5 MHz 12.5 *mm* diameter transducers. In the Rayleigh wave experiments 1 MHz 25 *mm* diameter and 10 MHz 12.5 *mm* diameter transducers on angled wedges were used. Fig. 2 shows the position of the transducers and the wedges in the Rayleigh wave experiments where they were set 12 *cm* apart. The tensile specimens were loaded in a 300 *kip* Universal Testing Machine with 'valve'-control. In the absence of strain control, partial unloading of the specimens was observed during loading in both the initial yield plateau and in the strain hardening regime. A representative stress-strain diagram for a thin specimen is shown in Fig. 3.

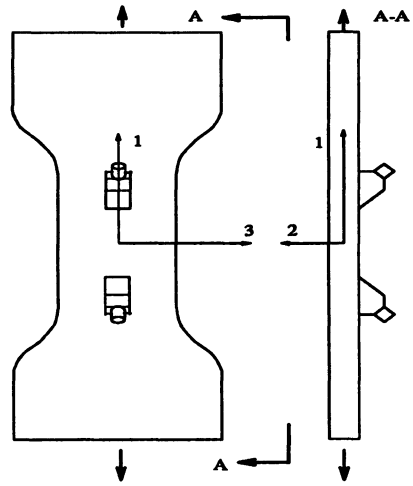

Figure 2: Schematics of tensile test specimen and ultrasonic instrumentation.

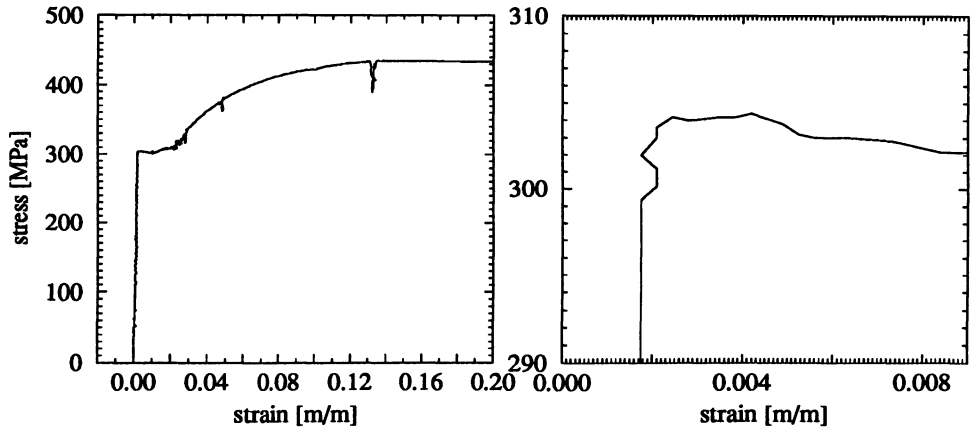

Figure 3: Stress-strain diagram of direct tension test, A-36 steel specimen.

Table 1: Comparison of theoretical elasto-plastic wave speeds with the ultrasonic test results after normalization by the elastic wave speeds c_{ql}^{el}, c_{qt}^{el}.

α	c_{ql}^{ep}	c_{qt}^{ep}	$c_{ql}^{exper}(\alpha)$	$c_{qt}^{exper}(\alpha)$
90^o	$0.95\ c_{ql}^{el}$	$1.00\ c_{qt}^{el}$	$1.00 c_{ql}^{el}$	–
45^o	$0.98\ c_{ql}^{el}$	$0.47\ c_{qt}^{el}$	–	$0.99 c_{qt}^{el}$

Longitudinal and Shear Wave Experiments

Table 1 summarizes the theoretical values for elasto-plastic loading waves for comparison with the measured velocities of quasi-longitudinal waves propagating in directions 2 and 3, and the quasi-transverse shear waves propagating at an angle $\alpha \approx 45^0$ with the x_1-axis. The measured velocities (Table 1) show little decrease when compared with the elastic wave velocities and do not match the theoretical predictions for the effects of elasto-plastic loading waves contrary to the nonlinear effects reported in ref. [3, 4]. This indicates that plastic loading waves could not be be discerned from arrival time measurements on one hand, and that elastic unloading was primarily observed because of early localization after the upper yield limit was reached. Enlarging the yield response in the right plot of Fig. 3 reveals that the transition from elasticity to plastic yielding is taking place very abruptly, within the upper and lower yield limit, quite opposite to the Maraging steel used in ref. [5] exhibiting continuous hardening. The transition to the lower yield limit is accompanied by softening at a tangent modulus which approaches the critical softening modulus for discontinuous bifurcation, $[h < h_{cr} = -E/12]$. The initially continuous plastic deformation field is therefore transformed into a narrow shear band due to localization. On the basis of the small change in the ultrasonic velocity detected in the measurements, the thickness of that plastic failure zone must be very small, possibly of the order of the mean grain size, $[\approx 0.02mm]$. Consequently, we conclude that in these experiments the ultrasonic waves propagates through an elastically unloading material and encounters a highly localized zone of 'plastified' interface material. Thereby, the elastic material properties show very little degradation indicating that elastic damage remains negligible due to elastic-plastic coupling.

Rayleigh Wave Experiments

Pairs of transducers were set on one side of samples such that Rayleigh waves travel across the expected deformation zone. The relative amplitudes of the Rayleigh waves and the stress level reached during uniaxial loading are shown in Fig. 4 . The data are normalized against the measured amplitude at the beginning of the test. All Rayleigh wave experiments did exhibit a significant drop in the amplitude of the transmitted wave when the material reached the yield limit. Fig. 4 also depicts the change of relative amplitude of the transmitted shear wave which shows very similar behavior as the amplitude in Rayleigh wave experiments. After sustained yielding, the amplitude rebounds in the data shown in Fig. 4, but never recovers fully to the initial value before localization during plastic yielding. Note that the transducers had to be removed from the specimen at the onset of necking before the tensile specimen experienced fracture.
The amplitude drop in the transmitted Rayleigh waves is attributed to the formation of an 'interface' zone, in which the plastic deformations are trapped resulting in a change of texture. The waves are partially reflected and mode converted as shown in Fig. 5. The thickness, inclination and material properties in the 'interface layer' all influence the transmission coefficient. Such interfaces and Rayleigh wave interactions are encountered in a range of physical systems that vary from fault-lines in geophysics to diffusion bonded interfaces inspected via acoustic microscopy [6]. The arrival times of the transmitted Rayleigh waves can be seen in the waterfall plots in Fig. 6. A distinct change of slope occurs at the onset of plastic yielding, and another one at the onset of plastic hardening.

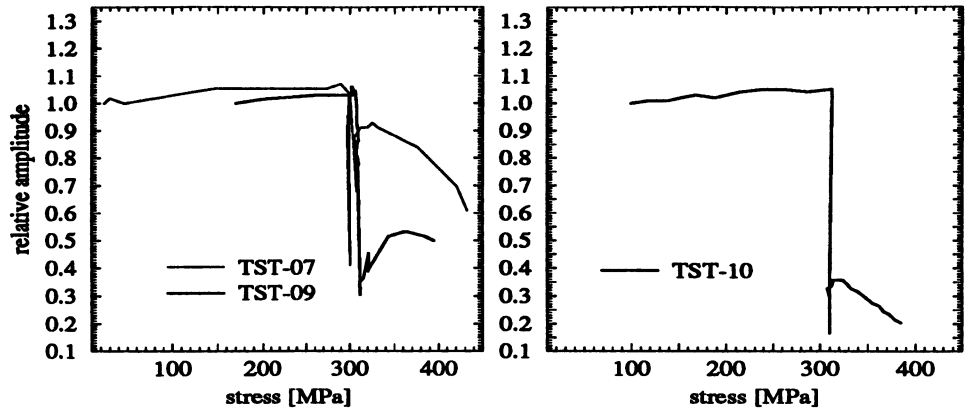

Figure 4: Examples of normalized Rayleigh wave (left) and Shear wave (right) amplitudes shown against sample stress level.

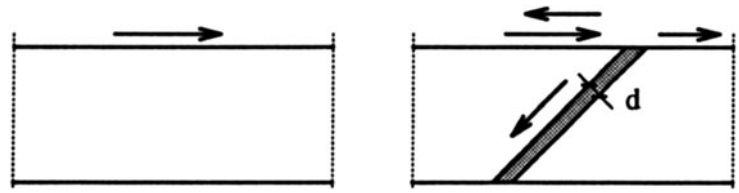

Figure 5: Formation of localized interface due to discontinuous bifurcation.

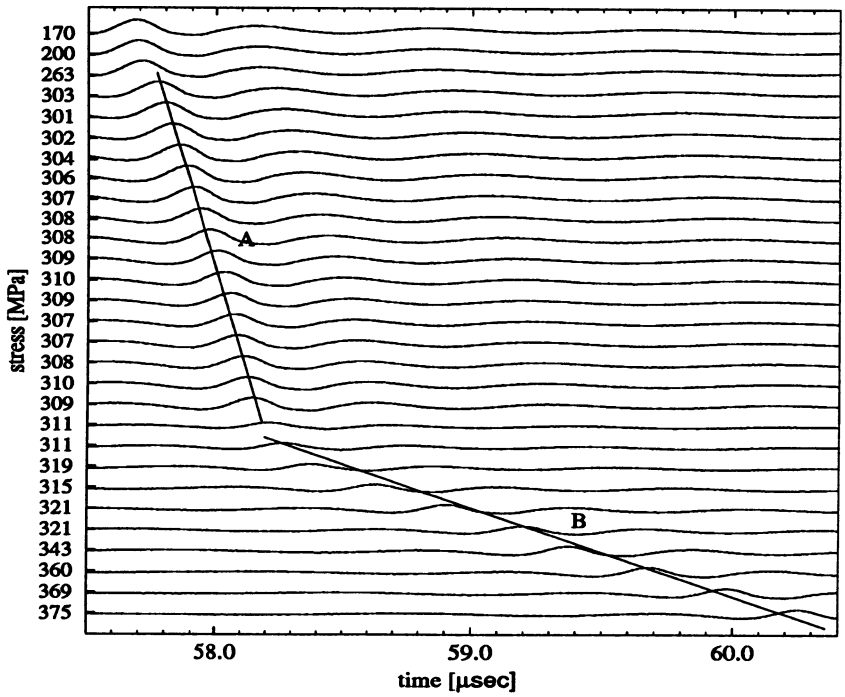

Figure 6: Transmitted Rayleigh wave arrival time changes at different stress levels.

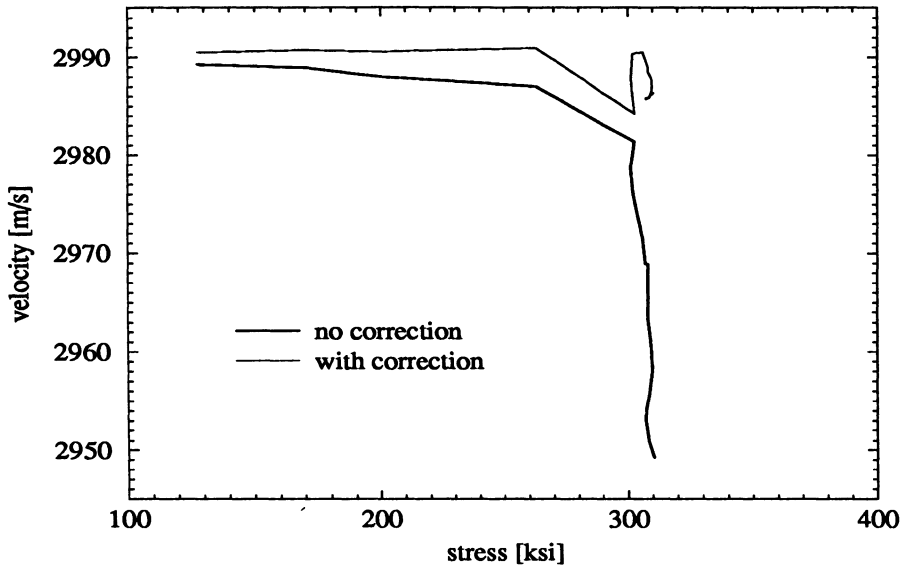

Figure 7: Variation of Rayleigh wave velocity with increasing stress level.

Considering the elongation of the tensile test region between the transducers the correction of the pathlength to the velocity data leads to the plot shown in Fig. 7. In view of the arrival time measurements with a resolution of $\pm 5nsec$ the actual change of Rayleigh wave velocities may be considered negligible. This leads to the conclusion that the lack of velocity drop is a manifestation of the specimen which is unloading elastically except for the localized 'interface' layer which is loading plastically. The orientation of the localized interface layer in Fig. 8 is aligned with the direction of the discontinuity surface which preconditions the ultimate failure mode of ductile fracture. Actually, there is also a second possible interface oriented at $(-\alpha)$ with respect to the x_1-axis, which is omitted in Fig. 8 for the sake of clarity. Moreover, the in-plane Lüder bands, which appear in very thin plane stress specimens at the angle $\alpha = \pm 35.26^0$ with the x_3-axis, see e.g. [1], do not develop because of the fairly thick specimen geometry.

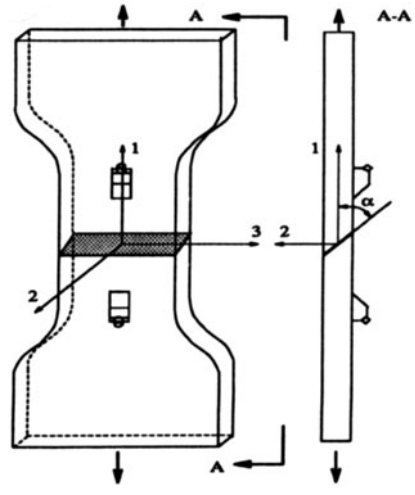

Figure 8: Orientation of localized interface layer in uniaxial tension.

CONCLUSIONS

The results of the ultrasonic experiments on the steel specimens loaded into the plastic yield regime indicate that the structural (A-36) steel undergoes a sudden transition from linear elastic behavior to plastic yielding with little changes of the (elastic) ultrasonic wave speeds. Early localization introduces a spatial discontinuity which transforms the uniformly stretched specimen into a heterogeneous structure with a plastic interface. The large jumps in transmitted Rayleigh wave amplitudes signal the formation of a localized shear band, while the accompanying reduction of Rayleigh wave velocity remains very small indicating negligible elastic degradation due to plastic yielding. It is expected that the ultrasonic experiments can be developed to characterize the interface properties of load induced shear bands.

ACKNOWLEGEMENTS

The first and third authors thank the National Science Foundation for the partial support under grant MSS-9103589 to the University of Colorado at Boulder. The authors wish to acknowledge the help of Lee Winkler who assisted with the ultrasonic experiments.

REFERENCES

1. Anand, L., Spitzig, W. A., "Initiation of Localized Shear Bands in Plane Strain", Journal of the Mechanics and Physics of Solids, Vol. 28, 113-128, 1980.
2. Auld, B.A., "Acoustic Fields and Waves in Solids", Krieger Publ. Co. Malabar FL., 1990.
3. Eagle, D. M., Bray, D.E., "Measurement of acoustoelastic and third-order elastic constants for rail steel", Journal of Acoustical Society of America, Vol.60, 741-744, 1976.
4. Hughes, D. S., Kelly, J.L., "Second Order Elastic Deformation of Solids", Physical Review, Vol 29, 1145-1149, 1953.
5. Ottosen, N. and Runesson, K., "Acceleration Waves in Elasto-Plasticity", International Journal of Solids and Structures, Vol. 28, 135-159, 1992.
6. Som, A.K., Bond, L.J. and Taylor, K.J., "Characterization of Diffusion Bonds Using an Acoustic Microscope ", Review of Progress in Quantitative NDE, Vol. 103., 1391-1398, 1991.
7. Willam, K., Sobh, N., and Sture, S., "Elastic-Plastic Tangent Operators: Localization Study on the Constitutive Level and the Finite Element Level", Advances in Inelastic Analysis, ASME-WAM'87, AMD Vol. 88, S. Nakazawa, K. Willam and N. Rebelo Eds., ASME New York, 107-126, 1987.